

Optimized Effective Potential made simple: Orbital functionals, orbital shifts, and the exact Kohn-Sham exchange potential

Stephan Kümmel and John P. Perdew
*Department of Physics and Quantum Theory Group,
 Tulane University, New Orleans, Louisiana 70118, USA*
 (Dated: October 24, 2018)

The optimized effective potential (OEP) is the exact Kohn-Sham potential for explicitly orbital-dependent energy functionals, e.g., the exact exchange energy. We give a proof for the OEP equation which does not depend on the chain rule for functional derivatives and directly yields the equation in its simplest form: a certain first-order density shift must vanish. This condition explains why the highest-occupied orbital energies of Hartree-Fock and exact-exchange OEP are so close. More importantly, we show that the exact OEP can be constructed iteratively from the first-order shifts of the Kohn-Sham orbitals, and that these can be calculated easily. The exact exchange potential $v_x(\mathbf{r})$ for spherical atoms and three-dimensional sodium clusters is calculated. Its long-range asymptotic behavior is investigated, including the approach of $v_x(\mathbf{r})$ to a non-vanishing constant in particular spatial directions. We calculate total and orbital energies and static electric dipole polarizabilities for the sodium clusters employing the exact exchange functional. Exact OEP results are compared to the Krieger-Li-Iafrate (KLI) and local density approximations.

PACS numbers: 71.15.Mb, 31.15.Ew, 36.40.-c, 73.22.-f

Physical Review B

I. INTRODUCTION

Density functional theory (DFT) in general and the Kohn-Sham scheme in particular are among the most important tools for electronic structure calculations. This success is based on a rigorous foundation in terms of the Hohenberg-Kohn theorem on the one hand¹, and increasingly sophisticated approximations to the exchange-correlation functional E_{xc} on the other. The local density approximation (LDA)² proved to be of far greater applicability than originally expected. Its great advantages are simplicity and reliability in the sense that its shortcomings are qualitatively predictable, but the price to be paid is limited accuracy. Generalized gradient approximations (GGA's)^{3,4,5,6} improved accuracy to a level that made DFT useful for many chemical applications. But despite their many successes, GGA's cannot be regarded as the final stage of functional development⁷. Further improvements in accuracy are expected from functionals that include partial or full exact exchange. Global^{8,9,10,11,12} and local¹³ hybrids and hyper-GGA's^{7,14} fall into this class.

Using the exact exchange energy in DFT calculations is promising from many points of view. Full exact exchange cancels the spurious Hartree self-interaction energy, curing in a systematic way one of the most notorious DFT problems. It leads to the correct high-density limit¹⁵, which is exchange dominated. Great improvements in the Kohn-Sham eigenvalue spectrum^{16,17}, semiconductor bandstructure and excitations^{18,19,20,21} and nonlinear optical properties²² have been reported using the exact exchange energy. The exact exchange functional also leads to the correct asymptotic ($r \rightarrow \infty$) behavior of the Kohn-Sham potential, which turns out to show surprising features not present in any of the common approximations, as discussed in Refs. 16,23 and below. Finally, the idea

of incorporating one more known exact ingredient into the energy functional is appealing in its own right.

But the goal of using the exact exchange energy or, more generally, any orbital functional self-consistently in Kohn-Sham calculations raises the question of how to construct the corresponding exchange-correlation potential. E_{xc} is still implicitly a functional of the density, but explicitly only its dependence on the set of occupied Kohn-Sham orbitals is known. Thus, calculating the corresponding exchange-correlation potential $v_{xc}(\mathbf{r}) = \delta E_{xc}[n]/\delta n(\mathbf{r})$ cannot be done straightforwardly by explicitly taking the functional derivative with respect to the density $n(\mathbf{r})$. Instead, the potential must be calculated from the optimized effective potential (OEP) integral equation^{24,25,26}. This approach is size-consistent if the orbital functional is invariant under unitary transformations of the occupied orbitals and is not too radically nonlocal²⁷. Size consistency is achieved for exact exchange, hybrid functionals^{8,9,10,11,12,13}, meta-GGA's^{28,29} and hyper-GGA's^{7,14}.

Due to its complexity, direct solutions of the OEP integral equation so far have been restricted to effectively one-dimensional systems with spherical symmetry^{25,30,31,32,33,34,35,36}, and the calculations for finite systems have been based on the program developed in Ref. 25. Hopes are low to generalize this approach to higher dimensions. The OEP for three-dimensional systems has been constructed by directly evaluating the response function using basis sets^{18,19,37,38,39}. This approach has proven successful, but requires considerable technical expertise: Summing over not only occupied but also unoccupied Kohn-Sham orbitals is required, and the necessary inversion of the response function can be cumbersome. And while the OEP total energy can be accurately obtained, the potentials and Kohn-Sham eigenvalues for finite systems may suffer from basis-set lim-

itations. A detailed discussion of the method and its limitations can be found in Refs. 40,41,42. Alternatively, the short-range part of the potential itself has been expanded in a basis set and the expansion coefficients chosen to minimize the total energy^{43,44,45}. This approach is appealing because of its directness. But the $-e^2/r$ -decay that the OEP is thereby forced to take everywhere in the asymptotic region of a finite system has to be reconsidered in the light of new conclusions about the asymptotic behavior of $v_x(\mathbf{r})$ presented in Refs. 16,23 and discussed below. Also, the method is hard to implement within fully numerical schemes for electronic structure calculations, and those continue to grow in importance^{46,47,48}.

In this manuscript we discuss how the OEP can easily be constructed from the first-order orbital shifts that have been introduced into OEP theory to justify the KLI approximation³⁰. We first present in Section II a new proof for the OEP equation that explains why this complicated equation can be cast in a simple form. In Section III we compare and contrast Hartree-Fock theory and exact-exchange OEP. Different methods to construct the OEP from the orbital shifts are analyzed in Section IV, together with indicators for the accuracy of an OEP solution. The exact-exchange OEP for spherical atoms and three-dimensional sodium clusters is calculated. Its long-range asymptotic behavior is investigated in Section V. We show that the behavior $\lim_{r \rightarrow \infty} v_x(\mathbf{r}) = -e^2/r + C$, with $C \neq 0$ on nodal surfaces of the highest occupied Kohn-Sham orbital, is a common situation for metal clusters. Finally, in Section VI we calculate the static electric polarizability for the neutral, even-electron clusters $\text{Na}_2 - \text{Na}_{10}$ in the exchange-only approximation, and compare LDA, KLI and exact OEP results.

II. THE OEP EQUATION IN TERMS OF THE FIRST-ORDER DENSITY SHIFT

As shown by Krieger, Li and Iafrate³⁰ and further clarified by Grabo, Kreibich, Kurth and Gross³⁶, the OEP integral equation for the spin-dependent exact Kohn-Sham exchange-correlation potential $v_{xc\sigma}(\mathbf{r})$ can be written in a form that takes a very simple interpretation. At the end of a long argument involving repeated application of the chain rule for functional derivatives and linear response theory, the OEP equation is written in the form

$$\sum_{i=1}^{N_\sigma} \psi_{i\sigma}^*(\mathbf{r}) \varphi_{i\sigma}(\mathbf{r}) + c.c. = 0. \quad (1)$$

Eq. (1) says that the optimum (i.e., yielding the lowest Kohn-Sham energy) potential $v_{xc\sigma}(\mathbf{r})$ to replace the orbital-dependent potential

$$u_{xci\sigma}(\mathbf{r}) = \frac{1}{\varphi_{i\sigma}^*(\mathbf{r})} \frac{\delta E_{xc}[\{\varphi\}]}{\delta \varphi_{i\sigma}(\mathbf{r})} \quad (2)$$

is the one that makes the change in the density vanish to first order in the perturbation

$$\Delta v_{i\sigma}(\mathbf{r}) = u_{xci\sigma}(\mathbf{r}) - v_{xc\sigma}(\mathbf{r}), \quad (3)$$

when this perturbation is applied to the Kohn-Sham system. The $\varphi_{i\sigma}(\mathbf{r})$ in Eq. (1) are the Kohn-Sham orbitals, i.e., the solutions of

$$\left(\hat{h}_{\text{KS}\sigma} - \varepsilon_{i\sigma}\right) \varphi_{i\sigma}(\mathbf{r}) = 0, \quad (4)$$

where $\hat{h}_{\text{KS}\sigma} = -(\hbar^2/2m)\nabla^2 + v_{\text{KS}\sigma}(\mathbf{r})$ is the Kohn-Sham Hamiltonian. The self-consistent Kohn-Sham potential

$$v_{\text{KS}\sigma}(\mathbf{r}) = v(\mathbf{r}) + v_{\text{H}}(\mathbf{r}) + v_{xc\sigma}(\mathbf{r}) \quad (5)$$

is the sum of the external potential $v(\mathbf{r})$, the Hartree potential $v_{\text{H}}(\mathbf{r}) = \int d^3r' e^2 n(\mathbf{r}')/|\mathbf{r} - \mathbf{r}'|$, and the spin-dependent exchange-correlation potential $v_{xc\sigma}(\mathbf{r}) = \delta E_{xc}[n]/\delta n_\sigma(\mathbf{r})$. ($v(\mathbf{r})$ can also depend upon σ , but usually does not.) $\psi_{i\sigma}(\mathbf{r})$ is the negative of the first-order perturbation-theory shift that results if $\varphi_{i\sigma}(\mathbf{r})$ is subjected to the perturbation of Eq. (3), i.e,

$$-\psi_{i\sigma}^*(\mathbf{r}) = \sum_{\substack{j=1 \\ j \neq i}}^{\infty} \frac{\int \varphi_{i\sigma}^*(\mathbf{r}') [u_{xci\sigma}(\mathbf{r}') - v_{xc\sigma}(\mathbf{r}')] \varphi_{j\sigma}(\mathbf{r}') d^3r'}{\varepsilon_{i\sigma} - \varepsilon_{j\sigma}} \varphi_{j\sigma}^*(\mathbf{r}). \quad (6)$$

For the sake of simplicity, we here assume non-degenerate orbitals. The extension to the degenerate case is unproblematic: As shown in Appendix B of Ref. 78, the restriction $j \neq i$ in the sum is to be replaced by $\varepsilon_{j\sigma} \neq \varepsilon_{i\sigma}$.

Note that, if the exact exchange energy

$$E_x[\{\varphi\}] = -\frac{e^2}{2} \sum_{\substack{i,j=1 \\ \sigma=\uparrow,\downarrow}}^{N_\sigma} \int \int \frac{\varphi_{i\sigma}^*(\mathbf{r}) \varphi_{j\sigma}^*(\mathbf{r}') \varphi_{j\sigma}(\mathbf{r}) \varphi_{i\sigma}(\mathbf{r}')}{|\mathbf{r} - \mathbf{r}'|} d^3r' d^3r, \quad (7)$$

is substituted for E_{xc} , then Eq. (2) just yields the orbital-dependent Hartree-Fock potential⁴⁹

$$u_{xio}(\mathbf{r}) = -\frac{e^2}{\varphi_{i\sigma}^*(\mathbf{r})} \sum_{j=1}^{N_\sigma} \varphi_{j\sigma}^*(\mathbf{r}) \int \frac{\varphi_{i\sigma}^*(\mathbf{r}') \varphi_{j\sigma}(\mathbf{r}')}{|\mathbf{r}' - \mathbf{r}|} d^3r'. \quad (8)$$

Eq. (1) is intuitively appealing for the following reasons: (1) It is a statement about the electron spin density, the central quantity of density functional theory. Going over from the optimized effective potential to the orbital-dependent potentials should not change the density much. In important limits (one- and two-electron ground states, and the uniform electron gas), the density should not change at all. (2) Once the OEP orbitals and orbital energies are fixed, Eq. (1) is homogeneous of degree one in the perturbation of Eq. (3), making $v_{xc\sigma}(\mathbf{r})$ a kind of average of the $u_{xci\sigma}(\mathbf{r})$. A simple average was proposed in Eq. (75) of Ref. 50, and averaged potentials are

popular in time-dependent DFT⁵¹. A sophisticated but still approximate average was proposed in Ref. 30. (3) Eq. (1) contains just enough information to define $v_{xc\sigma}(\mathbf{r})$ uniquely to within an additive constant, given the OEP orbitals and orbital energy differences: Imagine discretizing the \mathbf{r} space into a collection of M points $\mathbf{r}_1, \dots, \mathbf{r}_M$, and solving Eq. (1) as a set of $M - 1$ linear equations for the $M - 1$ unknowns $v_{xc\sigma}(\mathbf{r}_1), \dots, v_{xc\sigma}(\mathbf{r}_{M-1})$. Because the number of electrons cannot change, only $M - 1$ equations are linearly independent, leaving $v_{xc\sigma}(\mathbf{r}_M)$ as a free parameter. This parameter is normally chosen so that $\lim_{r \rightarrow \infty} v_{xc\sigma}(\mathbf{r}) = 0$.

The OEP equation has previously been investigated from different perspectives^{24,25,30,36,37,49,52,53,54}. But an equation as charmingly simple as Eq. (1) also deserves a simple proof. We provide one in the following. For notational simplicity, we drop the spin index σ in the rest of this section.

We start from a given expression for the total energy in terms of some set of orbitals $\{\phi\}$,

$$E_v^\alpha[\{\phi\}] = \frac{\hbar^2}{2m} \sum_{i=1}^N \int |\nabla \phi_i(\mathbf{r})|^2 d^3r + \int v(\mathbf{r})n(\mathbf{r}) d^3r + \frac{e^2}{2} \iint \frac{n(\mathbf{r})n(\mathbf{r}')}{|\mathbf{r} - \mathbf{r}'|} d^3r' d^3r + \alpha E_{xc}[\{\phi\}], \quad (9)$$

where

$$n(\mathbf{r}) = \sum_{i=1}^N |\phi_i(\mathbf{r})|^2. \quad (10)$$

The real parameter α is introduced for the sake of later arguments and can be set to 1 at the end. Based on Eq. (9), two different density functionals can be defined. The Kohn-Sham (i.e., OEP) functional is defined by choosing the $\{\phi\}$ to be the Kohn-Sham orbitals $\{\varphi\}$. This means that for a given density $n(\mathbf{r})$, we find a local potential $v_s(\mathbf{r})$ such that the solutions of the independent-particle Schrödinger equation

$$\left(-\frac{\hbar^2}{2m} + v_s(\mathbf{r})\right) \varphi_i(\mathbf{r}) = \varepsilon_i \varphi_i(\mathbf{r}) \quad (11)$$

yield the given density via Eq. (10). The orbitals are clearly functionals of $v_s(\mathbf{r})$ which is itself a functional of $n(\mathbf{r})$. The Kohn-Sham energy functional is then

$$E_v^{\text{OEP},\alpha}[n] = E_v^\alpha[\{\varphi[n]\}]. \quad (12)$$

Eq. (12) is minimized by the density $n^{\text{OEP},\alpha}(\mathbf{r})$, and this density is obtained by choosing for $v_s(\mathbf{r})$ the potential of Eq. (5) (with v_{xc} multiplied by α , see below). We define a second, ‘‘orbital’’ density functional

$$E_v^{\text{orb},\alpha}[n] = E_v^\alpha[\{\varphi^{\text{orb},\alpha}[n]\}] \quad (13)$$

as the energy obtained by evaluating Eq. (9) with a different set of orbitals $\{\varphi^{\text{orb},\alpha}\}$. The $\varphi_i^{\text{orb},\alpha}$ are defined

as those normalized linearly-independent orbitals that yield a given density via Eq. (10) and deliver the lowest extremum of $E_v^\alpha[\{\phi\}]$. (This definition is discussed in Appendix A). The density $n^{\text{orb},\alpha}(\mathbf{r})$ that minimizes $E_v^{\text{orb},\alpha}[n]$ results from the orbitals that are solutions of

$$\left(-\frac{\hbar^2}{2m} \nabla^2 + v(\mathbf{r}) + v_H(\mathbf{r}) + u_{xci}^{\alpha*}(\mathbf{r})\right) \varphi_i^{\text{orb},\alpha}(\mathbf{r}) = \varepsilon_i^{\text{orb},\alpha} \varphi_i^{\text{orb},\alpha}(\mathbf{r}). \quad (14)$$

The requirement of a local, orbital-independent potential in the definition of $E_v^{\text{OEP},\alpha}[n]$ can be understood as an additional constraint not present in $E_v^{\text{orb},\alpha}[n]$. Therefore, if we define a functional $A^\alpha[n]$ by

$$E_v^{\text{orb},\alpha}[n] = E_v^{\text{OEP},\alpha}[n] + A^\alpha[n], \quad (15)$$

we know that $A^\alpha[n] \leq 0$. From the minimum principle for $E_v^{\text{orb},\alpha}[n]$, and from the preceding statement, it is clear that

$$E_v^{\text{orb},\alpha}[n^{\text{orb},\alpha}] < E_v^{\text{orb},\alpha}[n^{\text{OEP},\alpha}] < E_v^{\text{OEP},\alpha}[n^{\text{OEP},\alpha}]. \quad (16)$$

For a given orbital functional, one achieves a lower energy with the orbital-dependent potentials than with the OEP.

Eq. (1) can now be deduced directly from the α -dependence of the two energy functionals. We first observe that

$$v_{xc}^{\text{OEP},\alpha}([n]; \mathbf{r}) = \alpha \frac{\delta E_{xc}^{\text{OEP}}[n]}{\delta n(\mathbf{r})}, \quad (17)$$

and

$$u_{xci}^\alpha(\{\phi\}; \mathbf{r}) = \alpha \frac{1}{\phi_i^*(\mathbf{r})} \frac{\delta E_{xc}[\{\phi\}]}{\delta \phi_i(\mathbf{r})}, \quad (18)$$

i.e., both the orbital-independent and the orbital-dependent potential depend linearly on α . We further observe that, in contrast to the $\varphi_i^{\text{orb},\alpha}(\mathbf{r})$, the Kohn-Sham orbitals for a given density do not depend on α : The Hohenberg-Kohn theorem tells us that, for a given density, $v_s(\mathbf{r})$ and thus the orbitals $\varphi_i(\mathbf{r})$ are uniquely fixed. Finally, we observe that for $\alpha = 0$, the functionals Eq. (12) and Eq. (13) are trivially identical. (Thus, in Eq. (20) below, $E_v^{\text{orb},0}[n] = E_v^{\text{OEP},0}[n]$.)

From the second observation and Eq. (9) one deduces that, for fixed external potential $v(\mathbf{r})$ and fixed density $n(\mathbf{r})$, the α -dependence of the OEP-functional is

$$E_v^{\text{OEP},\alpha}[n] = E_v^{\text{OEP},0}[n] + \alpha E_{xc}[\{\varphi[n]\}]. \quad (19)$$

In contrast, $E_v^{\text{orb},\alpha}[n]$ in general will not have such a simple dependence on α since the $\varphi_i^{\text{orb},\alpha}$ for a given density will change with α . Thus, the power series

$$E_v^{\text{orb},\alpha}[n] = E_v^{\text{orb},0}[n] + \alpha E_{v,1}^{\text{orb}}[n] + \alpha^2 E_{v,2}^{\text{orb}}[n] + \dots, \quad (20)$$

where formally $E_{v,1}^{\text{orb}}[n] = (\partial E_v^{\text{orb},\alpha}[n]/\partial \alpha)|_{\alpha=0}$, etc., will have non-vanishing terms beyond the one linear in α .

However, the crucial fact to note is that the term linear in α is the same in $E_v^{\text{OEP},\alpha}[n]$ and $E_v^{\text{orb},\alpha}[n]$: At $\alpha = 0$ (Hartree approximation), the orbitals are the same, i.e., $\varphi_i^{\text{orb},0}(\mathbf{r}) = \varphi_i(\mathbf{r})$, and we know that there can be no first-order change in $E_v^{\text{orb},\alpha}[n]$ due to a change in the orbitals, because we defined the $\varphi_i^{\text{orb},\alpha}(\mathbf{r})$ as extremizing orbitals. Therefore, $E_{v,1}^{\text{orb}}[n] = E_{\text{xc}}[\{\varphi[n]\}]$.

This means that the functional $A^\alpha[n]$ of Eq. (15) vanishes to linear order in α . It is then intuitively clear that the densities that minimize $E_v^{\text{orb},\alpha}[n]$ and $E_v^{\text{OEP},\alpha}[n]$ must also be the same to linear order in α . In other words, the difference to first order in α between $n^{\text{orb},\alpha}(\mathbf{r})$ and $n^{\text{OEP},\alpha}(\mathbf{r})$ must vanish, and, because of Eqs. (17) and (18), this difference is just given by the left-hand side of Eq. (1). A detailed version of these arguments is presented in Appendix B.

Note that the determinant of orbitals satisfying Eqs. (11) or (14) and achieving the lowest total energy need not necessarily satisfy the Aufbau principle, but might have unoccupied orbitals with orbital energies lying below occupied ones. Note further that, in the absence of a magnetic field, all the orbitals can be chosen to be real.

III. HARTREE-FOCK VS. EXCHANGE-ONLY OEP

As an important example of the ideas of Section II, let $E_{\text{xc}}[\{\phi\}]$ in Eq. (9) be the Fock exchange integral of the occupied orbitals of Eq. (7). Then the lowest extremum over linearly-independent orbitals in the definition of $E_v^{\text{orb},\alpha}[n]$ becomes the minimum over orthonormal orbitals. For given external potential $v(\mathbf{r})$ and electron number N , the $\varphi_i^{\text{orb},\alpha=1}(\mathbf{r})$ are the canonical Hartree-Fock orbitals. $E_v^{\text{orb},\alpha=1}[n]$ is the density functional for the Hartree-Fock energy defined by the Levy constrained search^{55,56} (but not known as an explicitly calculable functional of the Kohn-Sham orbitals or of the density). Its minimizing density $n^{\text{orb},\alpha=1}(\mathbf{r})$ is the Hartree-Fock density, and $E_v^{\text{orb},\alpha=1}[n^{\text{orb},\alpha=1}]$ is the Hartree-Fock energy. The minimizing problem for this functional can be formulated within Kohn-Sham theory, but the resulting Kohn-Sham orbitals $\varphi_i([n^{\text{orb},\alpha=1}]; \mathbf{r})$ are *not* the Hartree-Fock orbitals, although both sets of orbitals yield the same density. The relation between Hartree-Fock theory and DFT has also been studied in Ref. 57.

On the other hand, $E_v^{\text{OEP},\alpha}[n]$ is by definition²⁶ the exact exchange-only density functional of Kohn-Sham theory (an explicitly calculable functional of the Kohn-Sham orbitals, and one which defines the lower limit of the integrand in the coupling constant or adiabatic connection formula for $E_{\text{xc}}[n]$ ^{58,59}). The inequality following Eq. (15) shows that the Hartree-Fock exchange energy for a given density includes a negative contribution which from the exchange-only OEP perspective is a small part of the correlation energy^{60,61}. (The local density approximation to this part of the correlation energy vanishes, while its second-order gradient coefficient diverges²⁶, making it

very hard to approximate.) Since e^2 plays the same multiplicative role as α , the exact exchange energy of Kohn-Sham theory²⁶ for a given density is purely of order e^2 , while the Hartree-Fock exchange energy for the same density agrees with it to order e^2 , differing in order^{26,62} e^4 . Eq. (16) also shows that the Hartree-Fock total energy must be less than the total energy of the exact exchange-only OEP theory. These exact-exchange conclusions are not new²⁶, yet these subtle distinctions continue to cause some confusion.

The Hartree-Fock and exchange-only OEP minimizing densities for a given $v(\mathbf{r})$ also agree to order e^2 , differing from one another and from the correlated ground-state density in order e^4 . Since the highest-occupied orbital energy controls the asymptotic decay of the density, the highest occupied orbital energies must also agree to order e^2 with one another, and with minus the correlated first ionization energy^{63,64,65}. This helps to explain the observed⁶⁶ but previously unexplained (except by Eq. (24) below) closeness of these quantities.

Given $v(\mathbf{r})$, the Hartree-Fock and exchange-only OEP orbitals and other orbital energies differ in order e^2 . A good approximation to the occupied Hartree-Fock orbitals can be achieved by a unitary transformation of the occupied canonical OEP orbitals⁴¹. In particular, after mixing in the highest occupied OEP orbital, all the canonical Hartree-Fock orbitals so approximated will decay asymptotically with the same exponent. However, exact agreement is not expected even to order e^2 , since Eq. (6) shows that to order e^2 each *exact* canonical Hartree-Fock orbital is a superposition of all the exact-exchange occupied *and unoccupied* OEP orbitals. Thus, for a given $v(\mathbf{r})$, the Hartree-Fock and exchange-only OEP Slater determinants (which are invariant under unitary transformations of their occupied orbitals) also differ to order e^2 , and only the Hartree-Fock determinant agrees to order e^2 with the singles-only configuration interaction expansion of the correlated many-electron wavefunction (Brillouin's theorem⁶⁷).

IV. ITERATIVE SOLUTION OF THE OEP EQUATION

A. Constructing the OEP from the orbital shifts

The fact that the OEP can be expressed solely in terms of the occupied Kohn-Sham orbitals and their first-order shifts leads to a simple scheme for its construction. As a straightforward result from first-order perturbation theory, the partial differential equations

$$(\hat{h}_{\text{KS}\sigma} - \varepsilon_{i\sigma})\psi_{i\sigma}^*(\mathbf{r}) = -[v_{\text{xc}\sigma}(\mathbf{r}) - u_{\text{xc}i\sigma}(\mathbf{r}) - (\bar{v}_{\text{xc}i\sigma} - \bar{u}_{\text{xc}i\sigma})]\varphi_{i\sigma}^*(\mathbf{r}) \quad (21)$$

for the orbital shifts $\psi_{i\sigma}(\mathbf{r})$ are obtained, where $\bar{v}_{\text{xc}i\sigma} = \int \varphi_{i\sigma}^*(\mathbf{r})v_{\text{xc}\sigma}(\mathbf{r})\varphi_{i\sigma}(\mathbf{r})d^3r$ and $\bar{u}_{\text{xc}i\sigma} = \int \varphi_{i\sigma}^*(\mathbf{r})u_{\text{xc}i\sigma}(\mathbf{r})\varphi_{i\sigma}(\mathbf{r})d^3r$. (Note that the same equa-

tions can be obtained by other arguments^{30,36}). By solving Eq. (21) for $v_{\text{KS}\sigma}\psi_{i\sigma}^*$, inserting the result into Eq. (1) multiplied by $v_{\text{KS}\sigma}(\mathbf{r})$, and solving for $v_{\text{xc}\sigma}$, the exact exchange-correlation potential can be expressed explicitly in terms of only the occupied Kohn-Sham orbitals and their shifts^{30,36}:

$$v_{\text{xc}\sigma}(\mathbf{r}) = \frac{1}{2n_{\sigma}(\mathbf{r})} \sum_{i=1}^{N_{\sigma}} \left\{ |\varphi_{i\sigma}(\mathbf{r})|^2 [u_{\text{xc}i\sigma}(\mathbf{r}) + (\bar{v}_{\text{xc}i\sigma} - \bar{u}_{\text{xc}i\sigma})] + \varphi_{i\sigma}(\mathbf{r}) \left[\left(\frac{\hbar^2}{2m} \nabla^2 + \varepsilon_{i\sigma} \right) \psi_{i\sigma}^*(\mathbf{r}) \right] \right\} + c.c. \quad (22)$$

Invoking Eq. (1) once more, the last term can be rewritten to obtain the expression from which the KLI approximation – neglecting the terms involving the $\psi_{i\sigma}^*(\mathbf{r})$ – has been justified as a mean-field approximation^{30,36}:

$$v_{\text{xc}\sigma}(\mathbf{r}) = \frac{1}{2n_{\sigma}(\mathbf{r})} \sum_{i=1}^{N_{\sigma}} \left\{ |\varphi_{i\sigma}(\mathbf{r})|^2 [u_{\text{xc}i\sigma}(\mathbf{r}) + (\bar{v}_{\text{xc}i\sigma} - \bar{u}_{\text{xc}i\sigma})] - \frac{\hbar^2}{m} \nabla \cdot [\psi_{i\sigma}^*(\mathbf{r}) \nabla \varphi_{i\sigma}(\mathbf{r})] \right\} + c.c. \quad (23)$$

Since the potential $v_{\text{xc}\sigma}(\mathbf{r})$ of Eq. (23) is fixed only up to an additive constant, one is at liberty to choose one of the constants $\bar{v}_{\text{xc}i\sigma} - \bar{u}_{\text{xc}i\sigma}$ freely. The usual choice is^{30,36}

$$\bar{v}_{\text{xc}N_{\sigma}\sigma} - \bar{u}_{\text{xc}N_{\sigma}\sigma} = 0, \quad (24)$$

to make the potential vanish at infinity. We will discuss this point in greater detail in Section V.

Together with the orthogonality condition $\int \psi_{i\sigma}^*(\mathbf{r})\varphi_{j\sigma}(\mathbf{r})d^3r = 0$ that follows from Eq. (6), Eq. (21) uniquely determines the orbital shifts. In case of degeneracies, the orthogonality condition reads $\int \psi_{i\sigma}^*(\mathbf{r})\varphi_{j\sigma}(\mathbf{r})d^3r = 0$ for all pairs (i, j) with $\varepsilon_{i\sigma} = \varepsilon_{j\sigma}$. In Ref. 23 it was demonstrated that the $\psi_{i\sigma}^*(\mathbf{r})$ can easily be calculated from Eq. (21) and used to construct the OEP. The basic idea is to combine the Kohn-Sham equations (4) with the orbital shift equations (21) in a self-consistent iteration. This can be done in different ways. The first and obvious one consists of the following steps: Solve the Kohn-Sham equations with an approximation to the OEP, e.g., do a KLI calculation. Use the resulting $\varphi_{i\sigma}$ and $v_{\text{xc}\sigma}$ to construct the right-hand side of Eq. (21). Solve, e.g., by conjugate gradient iteration^{23,68}, for the orbital shifts. Insert the $\psi_{i\sigma}^*$ into Eq. (23) to obtain an improved approximation for $v_{\text{xc}\sigma}$. Then self-consistently solve the Kohn-Sham equations again for *fixed* $v_{\text{xc}\sigma}$ to obtain a new total energy and new eigenvalues. Repeat these steps until convergence is achieved.

This simple procedure only involves the occupied orbitals and their shifts. Instead of an integral equation, it only requires solving partial differential equations, which

can easily be done. We thus gain all the advantages of avoiding the explicit evaluation of the response function that are known from other areas of linear response theory^{69,70}.

In practice, a small modification of this algorithm is useful. After $v_{\text{xc}\sigma}$ has been updated, one need not directly go back to the Kohn-Sham equations. Instead, one can solve Eq. (21) again, keeping the left-hand side and the $\varphi_{i\sigma}$ fixed but evaluating the right-hand side with the new $v_{\text{xc}\sigma}$. Using this additional $(\psi_{i\sigma}^*, v_{\text{xc}\sigma})$ -cycle speeds up the convergence, and Eq. (21) is easier to solve than Eq. (4) since it is just a differential and not an eigenvalue equation. We discuss numerical aspects of the iteration and its convergence in detail in Appendix C. Here we just point out that the iteration converges very quickly: Starting, e.g. for the Be atom, from the KLI approximation and using 5 cycles per iteration, the total energy is correct after the first iteration and all eigenvalues after 5 iterations.

The iterative approach is also accurate. One criterion that indicates an accurate OEP can be inferred directly from Eq. (1). The function

$$S_{\sigma}(\mathbf{r}) = \sum_{i=1}^{N_{\sigma}} \psi_{i\sigma}^*(\mathbf{r})\varphi_{i\sigma}(\mathbf{r}) + c.c. \quad (25)$$

must vanish for the exact OEP. Therefore, the smaller the maximum value S_{max} that $S(\mathbf{r})$ takes in a given region of space, the more accurate is the potential. For the KLI potential of the Be atom, we find $S_{\text{max}} = 0.03 a_0^{-3}$. After 5 iterations with 5 cycles, S_{max} has fallen below $10^{-6} a_0^{-3}$. A second accuracy criterion is the exchange virial relation^{71,72}. It is slightly violated by the KLI approximation with a relative error of about 1%. By the time our iteration has refined all eigenvalues to 0.0001 hartree (0.1 mhar) accuracy, the error in the virial relation has been reduced to $10^{-4}\%$, and further iteration reduces it to $10^{-7}\%$. The method is thus at least as accurate as the direct solution of the integral equation^{31,32}.

However, applied to finite systems, Eq. (23) has an unpleasant feature: The second term under the sum on the right-hand side must be divided by the density. While this is not a problem theoretically, it complicates the numerical evaluation of Eq. (23) for finite systems. Far away from the system the density decays exponentially, and numerically dividing by a rapidly vanishing function introduces inaccuracies. These inaccuracies in the asymptotic region can magnify during the iteration and, if not taken care off, can spoil the whole scheme. In Appendix C we discuss this problem in greater detail, together with strategies to overcome it. Here we want to focus on how it can be completely avoided.

For many numerical problems, iterative solution strategies can be designed in different ways⁶⁸. Therefore, there is no reason to believe that Eq. (23) is the only way that the information contained in the orbital shifts can be used. In fact, Eq. (25) suggests a very simple, pragmatic alternative: Since $S_{\sigma}(\mathbf{r})$ is an indicator for the er-

ror inherent in a given approximation to the OEP, we improve the given approximation by adding the corresponding $S_\sigma(\mathbf{r})$ to it:

$$v_{xc\sigma}^{\text{new}}(\mathbf{r}) = v_{xc\sigma}^{\text{old}}(\mathbf{r}) + cS_\sigma(\mathbf{r}). \quad (26)$$

The real parameter $c > 0$ with dimension energy times volume is introduced because $S_\sigma(\mathbf{r})$ is not an exact representation of the error but just an estimate. Since it is not guaranteed that the $v_{xc\sigma}^{\text{new}}(\mathbf{r})$ from Eq. (26) will obey Eq. (24), we enforce it explicitly by adding the constant $\bar{u}_{xcN_\sigma\sigma} - \int \varphi_{N_\sigma}^*(\mathbf{r})v_{xc\sigma}^{\text{new}}(\mathbf{r})\varphi_{N_\sigma\sigma}(\mathbf{r})d^3r$ to $v_{xc\sigma}^{\text{new}}$ each time it has been updated via Eq. (26). (See Ref. 23 for an intuitive explanation of the same idea.)

Eq. (26), together with adding the constant, can replace the update of $v_{xc\sigma}$ via Eq. (23), and all the other steps described in the three paragraphs following Eq. (24) stay the same. As shown below, introducing c can be understood as replacing by a constant a term that requires dividing by the density. Doing so, we drop some information from the error feedback, and therefore the iteration converges somewhat slower than the direct iteration of Eq. (23). But with 10 $(\psi_{i\sigma}^*, v_{xc\sigma})$ -cycles per iteration, the total energies of the atoms Be, Ne, Na, Mg, and Ar converge within 0.1 mhar in 2, 2, 2, 5, and 7 iterations, respectively (and a larger number of cycles further reduces the number of necessary iterations). The computational effort is therefore only moderate. The OEP energies from our solution are identical to the ones found from the considerably more involved direct solution of the integral equation^{25,36}, and the iteration is as accurate (see Appendix C for tests).

This approach can be motivated further by rewriting Eq. (21) such that the left-hand side becomes $(\hbar^2/(2m)\nabla^2 + \varepsilon_{i\sigma})\psi_{i\sigma}^*$ and inserting the result into the right-hand side of Eq. (22) to obtain

$$v_{xc\sigma}(\mathbf{r}) = v_{xc\sigma}(\mathbf{r}) + \frac{v_{KS\sigma}(\mathbf{r})}{2n_\sigma(\mathbf{r})}S_\sigma(\mathbf{r}). \quad (27)$$

This is a trivial identity if $\varphi_{i\sigma}$ and $\psi_{i\sigma}^*$ are the orbitals and shifts corresponding to the true OEP. However, if $\varphi_{i\sigma}$ and $\psi_{i\sigma}^*$ have been calculated from an approximation to the OEP, then the second term on the right-hand side does not vanish and represents an error term. Its most important part is the function $S_\sigma(\mathbf{r})$ which by definition contains the information about where the OEP equation is violated. By subtracting the error term from the approximation, we get a better approximation. But we only want to subtract the part that is proportional to $v_{xc\sigma}$,

$$v_{xc\sigma}^{\text{new}}(\mathbf{r}) = v_{xc\sigma}^{\text{old}}(\mathbf{r}) - \frac{v_{xc\sigma}^{\text{old}}(\mathbf{r})}{2n_\sigma(\mathbf{r})}S_\sigma(\mathbf{r}), \quad (28)$$

because for stability reasons we do not want to change $v_{xc\sigma}$ too drastically in each iteration. (Subtracting the full term using v_{KS} would, e.g., introduce a very different length scale and the nuclear singularity into the iteration. Besides, in the neutral systems of interest here, v_{xc} dominates the asymptotics of v_{KS} .) We have tested Eq. (28)

for spherical atoms, and it converges nearly as quickly as the direct iteration of Eq. (23). But since Eq. (28) also requires dividing by the density, the simpler iteration based on Eq. (26) is more practical, in particular for the cluster calculations. Eq. (28) provides an interpretation for the constant c : It takes the role of an average value for $v_{xc\sigma}^{\text{old}}(\mathbf{r})/(2n_\sigma(\mathbf{r}))$. Since $v_{xc\sigma}$ is negative and we chose c to be positive, the signs in Eqs. (26) and (28) are opposite. In practice, the numerical value of c can be determined unproblematically by trial and error. For the systems we studied, we found c close to the values inferred from Eq. (28); see Appendix C.

B. OEP for Na clusters

Eq. (26) can very easily be employed in three-dimensional calculations and allows us to study the influence that the exact exchange functional has on non-spherical systems. The electrons in atoms are rather strongly localized. Metal clusters, and in particular sodium clusters, have a very different electronic structure with strongly delocalized valence electrons. They can thus be regarded as an ‘‘opposite’’ test case for the influence of exact exchange. Of particular interest is their static electric polarizability, which we will address in Section VI below.

We first calculated the ground-state properties of small sodium clusters using the exact exchange functional together with the exact OEP and with the KLI approximation, and for comparison also with LDA for exchange only (xLDA) and LDA for exchange and correlation⁷³. For reasons discussed in Section VI, we used the optimized cluster geometries and pseudopotential from Ref. 74,75. The results are summarized in Table I. For the smallest cluster Na_2 , which has one valence electron of each spin, the KLI approximation is exact. This is confirmed by the exchange virial relation: Whereas for all other clusters the virial relation is slightly violated by the KLI approximation with a relative error of about 0.5%, its relative error is only 10^{-6} for Na_2 . The total energies of all larger clusters are lower with the OEP than with the KLI potential, as required. The absolute average difference of 0.5 mhar indicates that KLI is a rather good approximation for the total energies. It should also be noted, however, that the relative error is considerably larger for the clusters than for the atoms. The differences between the Kohn-Sham eigenvalues obtained from OEP and KLI are larger than the differences in total energy, and there is a clear pattern: As for the atoms, the OEP raises the lowest occupied eigenvalues and lowers the highest occupied ones. Thus, the energy range of the occupied Kohn-Sham spectrum is up to 6% narrower in OEP than in KLI. This might well influence time-dependent DFT calculations to which the eigenvalues are an important ingredient. Comparing the results from the exact exchange functional to the xLDA results shows that, as expected, exact and local exchange lead

TABLE I: Absolute value of the total energy and lowest and highest occupied Kohn-Sham eigenvalue for small sodium clusters, in hartree, for exchange only OEP, KLI, and local exchange, and for local exchange and correlation⁷³. For the two-valence-electron system Na₂, the KLI potential is the exact OEP.

	Na ₂			Na ₄			Na ₆			Na ₈			Na ₁₀		
	-E	$-\varepsilon_L = -\varepsilon_H$		-E	$-\varepsilon_L$	$-\varepsilon_H$	-E	$-\varepsilon_L$	$-\varepsilon_H$	-E	$-\varepsilon_L$	$-\varepsilon_H$	-E	$-\varepsilon_L$	$-\varepsilon_H$
xOEP	0.3768	0.1701		0.7531	0.1762	0.1401	1.1421	0.1861	0.1496	1.5285	0.1954	0.1459	1.9082	0.1956	0.1263
xKLI	-	-		0.7528	0.1776	0.1394	1.1417	0.1871	0.1494	1.5282	0.1963	0.1458	1.9070	0.1965	0.1248
xLDA	0.3479	0.0874		0.7047	0.1123	0.0717	1.0810	0.1205	0.0824	1.4619	0.1331	0.0826	1.8257	0.1410	0.0664
LDA	0.4018	0.1135		0.8166	0.1384	0.0976	1.2511	0.1469	0.1085	1.6926	0.1596	0.1085	2.1169	0.1672	0.0926

to considerably different eigenvalue spectra: Exact exchange eigenvalues are more negative, and in particular the highest one is relatively much more negative. The total energy in xLDA is less negative than that with exact exchange, reflecting the well known effect that the local approximation underestimates the magnitude of the exchange energy. When local correlation is included, the local exchange error in the total energy is compensated to a good part. The eigenvalues, however, are still considerably smaller in absolute value even with correlation.

Finally, we investigate the orbital shifts $\psi_{i\sigma}^*(\mathbf{r})$. This can be done in a transparent way for Na₄: With two electrons of each spin, the KLI potential and OEP are already non-trivially different, yet we only need to look at two orbitals and shifts. The upper part of Fig. 1 shows the lower of the two Kohn-Sham orbitals as obtained from the KLI approximation and the OEP. The orbital is plotted for both potentials once along the y-axis and once along the z-axis. The ionic configuration of Na₄ and our labeling of axes is shown in Fig. 2. Clearly, the orbital obtained within KLI is very similar to the orbital from the exact OEP. The second Kohn-Sham orbital which is not shown in Fig. 1 can be described as a p_z orbital, i.e., it has a node in the x-y plane. The second KLI and OEP orbitals are also very similar. However, the conclusion that, therefore, the orbital shifts obtained from KLI and OEP should be very similar, too, is wrong. In the middle part of Fig. 1 the first orbital shift is shown along the z-axis. The shift calculated from the OEP via Eq. (21) shows a “dip” at the origin which is not seen in the shift corresponding to the KLI potential. And along the y-axis (lower part of Fig. 1), the shifts obtained from the KLI potential and the OEP are totally different: The KLI shift shows a pronounced central peak, whereas the OEP shift practically vanishes on the y-axis. The explanation for these somewhat surprising observations can be found directly in the OEP equation Eq. (1). As mentioned before, the x-y plane is a nodal plane for the higher of the two Kohn-Sham orbitals of Na₄. The lower orbital, however, does not vanish in the x-y-plane. Eq. (1) can therefore only be fulfilled in the x-y-plane if the orbital shift corresponding to the lower orbital vanishes in this plane. The KLI potential is only an approximation to the OEP, and therefore need not and, as seen in Fig. 1, does not fulfill Eq. (1) in the x-y-plane. The iteratively

constructed OEP, in contrast, makes the orbital shift vanish in the plane, as it should. The lower part of Fig. 1 thus once more confirms that we are indeed constructing the exact OEP. The reason for the pronounced difference between the OEP and KLI orbital shift is discussed in greater detail in Appendix D.

It remains to be explained why the orbital shift shown in the lower part of Fig. 1 vanishes perfectly between $y=-7 a_0$ and $z=+7 a_0$, but still shows a tiny bump at larger distances, a remnant from the KLI orbital shift. The reason is our iteration based on Eq. (26). It corrects the potential quickly in the energetically-important region where the orbitals and their shifts are appreciable. In the asymptotic region, however, $\varphi_{i\sigma}(\mathbf{r})$ and $\psi_{i\sigma}^*(\mathbf{r})$ decay exponentially, and consequently the potential is modified to a lesser extent. But why does this matter since it is believed that the KLI potential is asymptotically correct? The answer is that the KLI potential is asymptotically correct everywhere *except* on nodal surfaces of the highest-occupied orbital that extend out to infinity. On such nodal surfaces, a small difference between KLI potential and OEP is observed even in the asymptotic region, and it is this difference which gives rise to the above mentioned “bump”. This aspect will be discussed in greater detail in the next section. Here we just briefly want to mention that, if needed, the iteration based on Eq. (26) can be modified to yield quickly the correct asymptotic behavior also on the nodal surface: the constants $\bar{v}_{xc i\sigma} - \bar{u}_{xc i\sigma}$ which determine the asymptotic behavior (see below) only depend on the energetically-important region. Their values (and thereby the asymptotic limits of the exchange potential) are thus accurately known after just a few iterations, even when the potential converges slowly in the asymptotic region.

V. ASYMPTOTIC BEHAVIOR OF $v_x(\mathbf{r})$

The long-range asymptotic behavior of the exact exchange OEP can be inferred from Eq. (23). The first term in the sum over all occupied orbitals determines the asymptotics^{16,36}, since the highest-occupied orbital shift falls off faster than the highest-occupied orbital. The Kohn-Sham orbitals of a finite system decay exponentially like $\exp[-(-2m\varepsilon_{i\sigma}/\hbar^2)^{1/2}r]$, where r is the dis-

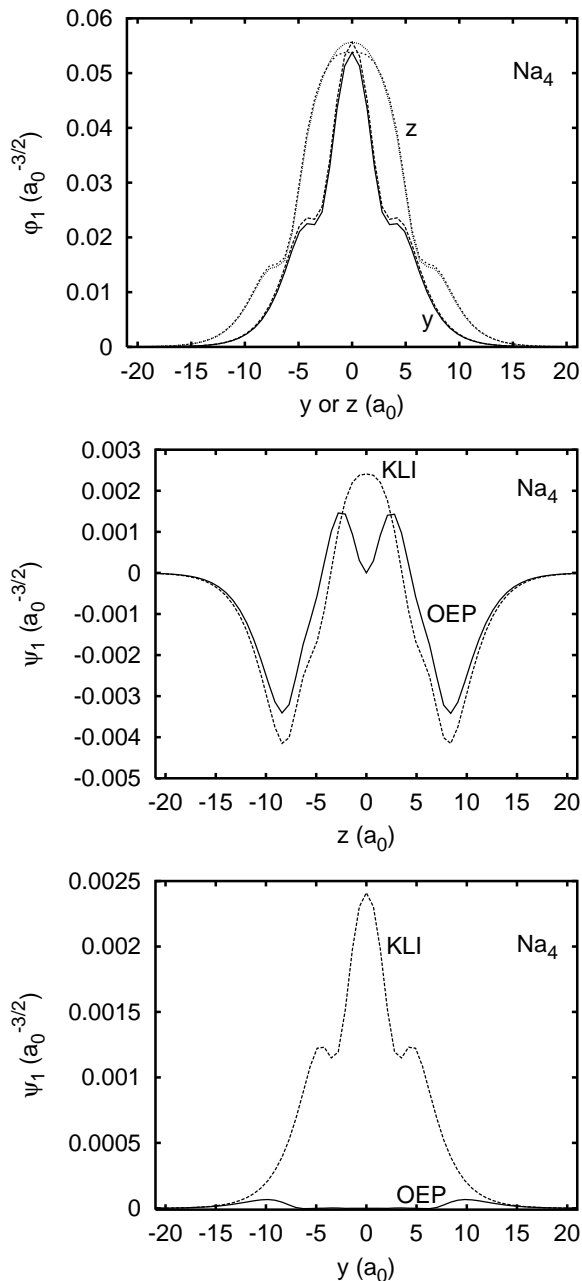


FIG. 1: The lowest Kohn-Sham orbital and corresponding orbital shift for Na_4 . Top: Full and long dashed: Orbital from OEP and KLI potential, respectively, along the y-axis. Short dashed and dotted: Orbital from OEP and KLI potential, respectively, along the z-axis. Middle: The corresponding orbital shifts plotted along the z-axis. Full: OEP, dashed: KLI. Bottom: Same orbital shifts along the y-axis. Full: OEP, dashed: KLI. See text for discussion.

tance from the system's center. This is a consequence of the locality of the Kohn-Sham potential and means that each orbital's decay is dominated by its own orbital energy. Therefore, the sum asymptotically will be dominated by the slowest-decaying orbital, which is the one with the highest orbital energy. Since $u_{xN_\sigma\sigma} \xrightarrow{r \rightarrow \infty} -e^2/r$,

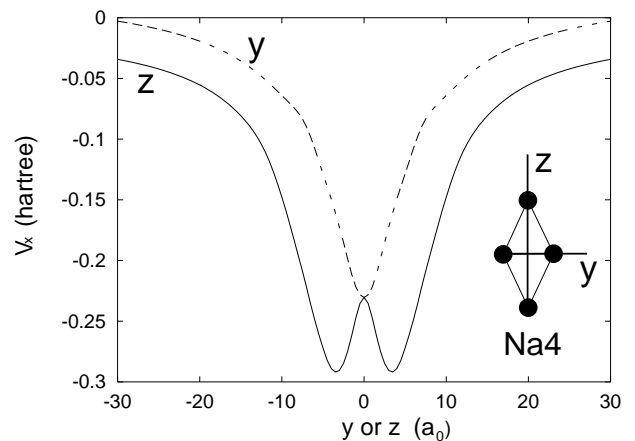


FIG. 2: The exact exchange potential of Na_4 in hartree along the z-axis (full line) and the y-axis (dashed line) in bohr a_0 . The potential goes to different asymptotic limits in different directions.

$v_x(\mathbf{r})$ for a finite system goes to zero like $-e^2/r$ in all regions of space that are dominated by the highest-occupied orbital density $n_{N_\sigma}(\mathbf{r}) = |\varphi_{N_\sigma}(\mathbf{r})|^2$. That the potential goes to zero and not some finite constant is due to Eq. (24). However, there may also be asymptotic regions of space where $n_{N_\sigma}(\mathbf{r})$ vanishes, but the orbital density of a lower occupied orbital M_σ does not. As pointed out in Ref. 16, this situation occurs whenever the highest occupied orbital has a nodal surface that extends out to infinity. In these regions, one can go through all the arguments used to derive the asymptotic behavior and replace $n_{N_\sigma}(\mathbf{r})$ by $n_{M_\sigma}(\mathbf{r})$. But the reference point for the potential was already fixed via Eq. (24). We cannot choose a second one, therefore there is no equivalent of Eq. (24) for the M_σ orbital. Consequently, the potential will asymptotically go to $C = \bar{v}_{xcM_\sigma\sigma} - \bar{u}_{xcM_\sigma\sigma}$, where in general $C \neq 0$. Thus, it must be concluded that the exact Kohn-Sham exchange potential can go to different asymptotic constants in different spatial directions.

In Ref. 30 this aspect of Eq. (23) was first discussed, but its consequences for the Kohn-Sham potentials of real systems were not considered. In Ref. 16 it was demonstrated that the effect indeed occurs for real systems, but the numerical calculations were restricted to the "localized Hartree-Fock" approximation to the OEP. Finally, in Ref. 23 and in this paper, we evaluate the exact OEP including the asymptotic region for realistic, three-dimensional systems and confirm the surprising asymptotic behavior of the exact exchange potential.

Fig. 2 shows the exchange-only OEP for the cluster Na_4 , the electronic structure of which was discussed in the previous section. The full line shows $v_x(\mathbf{r})$ along the z-axis. In this direction, the density is asymptotically dominated by the highest occupied orbital and the potential falls off like $-e^2/r$, as expected. The dashed line shows $v_x(\mathbf{r})$ along the y-axis. Clearly, the potential falls off in the same way, but tends to a different constant

C . We find $C = 0.0307$ har. This non-vanishing value for C is of course found only in the x-y-plane. Moving away from the origin at any low angle to this nodal plane, one eventually reaches a region where the highest-occupied orbital will dominate the density and $v_x(\mathbf{r})$ will tend to zero. A lower angle just means that the asymptotic region starts further away from the center of the cluster. But nevertheless, since the exchange potential is a continuous function of \mathbf{r} , the non-vanishing asymptotic constant has a substantial influence on $v_x(\mathbf{r})$ even outside of the nodal plane of the highest occupied orbital. To demonstrate this, we show in the lower half of Fig. 3 the exact exchange potential for Na_4 , and the potential from the local density approximation in the upper. For each point in the y-z-plane, the potential we calculated on a numerical grid is plotted as the “height”. The LDA-potential mirrors the density closely, so the ionic cores which cause “bumps” in the valence electron density show up in the LDA potential. We also observe the well-known effect that the LDA potential decays very quickly: it vanishes on the boundary of the plotted re-

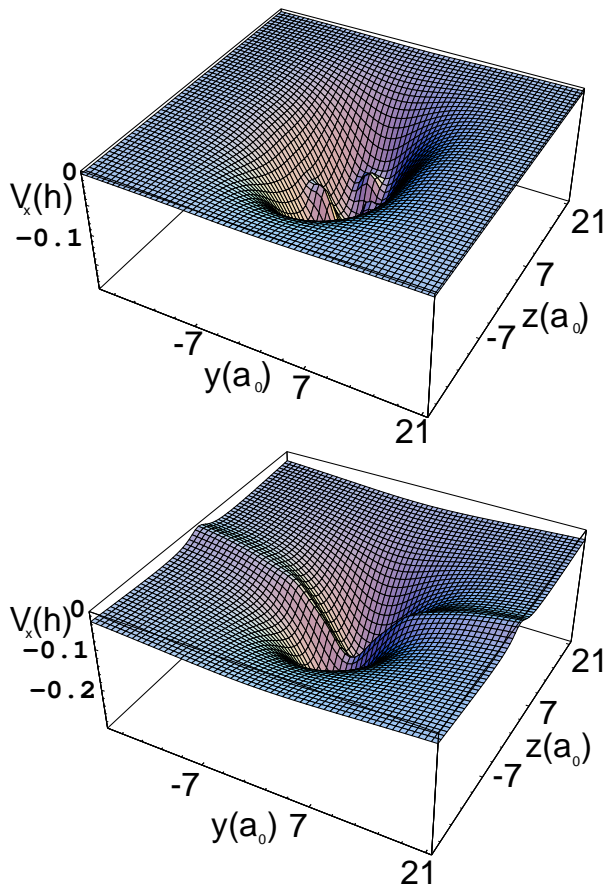


FIG. 3: The exchange potential “landscape” for Na_4 in the y-z plane: $v_x(\mathbf{r})$ in hartree defines the “height” at each spatial point (y,z) for fixed $x=0$. Upper: exchange-only LDA potential; lower: exact exchange potential (OEP). Note the greater depth, slower decay, and pronounced “ridge” seen in the OEP.

gion, whereas the exact exchange potential still takes a non-vanishing value there. But the most obvious difference between the exact and the local exchange potential is that the former shows a pronounced “ridge” running along the y-axis. This ridge is a consequence of the non-vanishing asymptotic constant: The potential has to go up to reach its correct value on the nodal surface. We find qualitatively the same behavior for all the clusters we studied here. For Na_6 and Na_8 , there are two degenerate highest orbitals, and the OEP goes to $C = 0.0378$ and $C = 0.0084$, respectively, on the z-axis. (We choose our Cartesian coordinates such that the axes are the principal axes of the cluster’s tensor of inertia, and z is the axis whose principal value differs most from the average. All constants are in har.) The relatively small constant for the “magic” Na_8 reflects the fact that the highest orbital is nearly degenerate with the two lower-lying ones. For Na_{10} , the situation is similar to Na_4 , with $C = 0.0107$ in the x-y-plane. Finally, it is clear from Eq. (23) that the asymptotic constants are qualitatively correct in the KLI potential. But KLI and OEP orbitals differ slightly, as shown in the previous section. Consequently, we find constants that differ by about 0.001 har in all cases we investigated.

The non-vanishing asymptotic constants are thus the rule, not the exception, and one may ask how this result can be true since there is a physical argument to explain the asymptotic behavior of the Kohn-Sham potential: An electron that wanders far out from a finite neutral system basically sees the attraction from the hole it leaves behind. Thus, the Kohn-Sham potential should fall off to $-e^2/r$ everywhere, without additional constants⁷⁶. However, appealing as this argument is, it cannot be applied to the Kohn-Sham potential. The Kohn-Sham potential is not a physical potential whose value we can measure. It is a mathematical construction, and therefore can have properties that physical potentials do not show. But of course the Kohn-Sham potential is a very clever mathematical construction, designed to yield from a simple procedure an accurate description of complicated quantities we can measure, like the ground-state energy of a many body system. Therefore, it is important to understand its features, in particular the surprising ones. The first and probably most extreme is the discontinuity of the Kohn-Sham potential as a function of electron number^{77,78,79}. The existence of non-vanishing asymptotic constants is a second one.

VI. STATIC ELECTRIC POLARIZABILITIES FROM THE EXACT EXCHANGE FUNCTIONAL

To demonstrate the importance of incorporating exact exchange into functionals, we investigate the static electric dipole polarizability. There has been a long-standing controversy about the influence of the long-range asymptotics of the Kohn-Sham potential and the self-interaction error on the optical properties of metal

clusters^{74,80,81,82,83,84,85,86,87,88}. The static electric dipole polarizability has been of particular interest: It was one of the earliest observables to give insight into the structure of clusters⁸⁹, its measurement gives information on the effects that govern cluster growth⁹⁰, and it may be used as an indicator for whether the bulk limit is reached⁹¹. The polarizability of small sodium clusters has been calculated before^{74,80,83,85,87,88}. It was found that, while local and semi-local density functionals yield polarizabilities in reasonable qualitative agreement with experiment, they do not lead to quantitative agreement. However, it has also been demonstrated^{92,93,94} that a finite cluster temperature greatly influences the static electric polarizability, mainly through the effect of thermal expansion⁹². The clusters' temperature in the experiments is presently not accurately known, but it is estimated to be high enough to account perhaps for all of the observed difference^{74,92,93}. Nevertheless, it is of great practical interest to obtain accurate theoretical values for the polarizability because the polarizability could then be used as a "thermometer" to estimate experimental cluster temperatures, as discussed in greater detail by Kronik and co-workers⁴⁷.

Our exact-exchange OEP calculations allow us to answer some of the questions related to the influence of self-interaction errors and long-range asymptotics that have been raised in the past. In the present study, our focus is on investigating these two effects by comparing LDA and exact-exchange results. In order to sort out the effects as clearly as possible, we want the valence electrons to move in exactly the same external potential for all E_{xc} functionals. Thus, we use the same pseudopotential and cluster geometries for different E_{xc} . For an accurate comparison with experimental data, a consistent exact-exchange pseudopotential^{20,95,96,97} should of course be used and the cluster structures re-optimized. But the comparison with experiment would also require inclusion of correlation effects. Since a correlation functional generally compatible with full exact exchange is not yet available, these aspects will have to be addressed in future work.

We calculated the mean static electric dipole polarizability $\bar{\alpha} = \text{tr}(\boldsymbol{\alpha})/3$ for the neutral sodium clusters with even electron numbers between 2 and 10, using the LDA-optimized geometries of Refs. 74,75. The polarizability tensor $\boldsymbol{\alpha}$ was obtained from the electric dipole moment $\mu_j(\mathbf{F}) = -e \int r_j n(\mathbf{r}, \mathbf{F}) d^3r$ by evaluating the definition $\alpha_{ij} = \lim_{F_i \rightarrow 0} \partial \mu_j / \partial F_i$, $i, j = x, y, z$, for a small but finite electrical field \mathbf{F} (see Ref. 74 for details, e.g., on the role of the ionic cores).

Table II summarizes the results of our calculations. We find that, for exact exchange and no correlation, the polarizabilities calculated using the exact OEP are consistently lower than the ones calculated from the KLI approximation. This is in agreement with our expectations, since the OEP yields lower total energies, i.e., binds the valence electrons more strongly than the KLI potential, and the valence electron density is thus harder to displace

by the electric field. It should be noted, however, that the difference between OEP and KLI polarizabilities is on the order of 1 %. By repeating our calculations for different electric field strengths and on different Cartesian grids with spacings between $0.5a_0$ and $0.8a_0$ and between 65 and 129 point in each spatial direction, we estimated the numerical accuracy of our calculations to be somewhat better than 1%. Thus, the inaccuracies that are introduced by using the KLI approximation are close to the numerical limits, showing once again that, for the present systems and observables, KLI is a good approximation to the OEP.

Compared to exchange-only LDA, the OEP yields polarizabilities which are on average a noticeable 7% lower. Again, this result can readily be understood: Local exchange makes a large self-interaction error, i.e., overestimates the electron-electron repulsion. This leads to a density that is too delocalized, which in turn results in too high a polarizability. The self-interaction error decreases with increasing electron delocalization, and the valence electrons in sodium are nearly free electrons. Therefore, we expect the largest self-interaction errors and differences between local and exact-exchange polarizabilities for the smallest clusters. This is confirmed by Table II. However, the fact that the difference falls from Na_2 to Na_8 , but increases somewhat from Na_8 to Na_{10} , shows that this argument seems to hold for the overall trend, but details in the electronic configuration also seem to matter.

Finally, comparing exact-exchange OEP to LDA for exchange and correlation, we find the surprising result that the polarizabilities are nearly the same. How can this be understood? The self-interaction error for local exchange and correlation together is smaller than for local exchange alone. So if inclusion of local correlation for the sodium clusters would lead to perfect cancellation of the self-interaction errors, then the fact that the polarizabilities are practically equal would not come as a surprise. However, the local correlation functional does not merely reduce the self-interaction error. Correlation functionals quite generally also describe short-range

TABLE II: Mean static electric dipole polarizability $\bar{\alpha}$ of Na clusters in \AA^3 for different approximations to E_{xc} and v_{xc} . Columns from left to right: exact exchange with exact OEP; exact exchange with potential in KLI approximation; LDA for exchange only; LDA⁷³ for exchange and correlation; relative difference in % between local and exact-exchange polarizabilities, $\Delta\alpha = \bar{\alpha}^{x,\text{LDA}} - \bar{\alpha}^{x,\text{OEP}}$.

Cluster	$E_x^{\text{ex,OEP}}$	$E_x^{\text{ex,KLI}}$	E_x^{LDA}	E_{xc}^{LDA}	$\Delta\alpha/\bar{\alpha}^{x,\text{OEP}}$
Na_2	36.9	36.9	40.4	37.1	9.5
Na_4	78.7	79.4	85.7	78.8	8.9
Na_6	107.6	108.3	115.0	107.3	6.7
Na_8	125.8	126.6	131.4	123.0	4.5
Na_{10}	158.7	160.8	168.4	157.3	6.1

Coulomb effects that lead to stronger binding. Thus, we expect that adding an appropriate correlation functional to the exact exchange will bind the valence electrons more strongly, yield a more compact density and thus lower the polarizability. Qualitatively, our results thus indicate that the LDA overestimates the polarizability. This conclusion, of course, is restricted to our special situation of fixed external potential. In future work we plan to investigate this question further by combining a newly developed, self-interaction-free meta-GGA for correlation⁹⁸ with the exact exchange functional.

VII. SUMMARY AND CONCLUSION

In summary, we have presented a new proof for the OEP equation that highlights the relationship between different density functionals (e.g., Hartree-Fock and exchange-only OEP) that can be defined from a given orbital expression for the energy. The proof explains why the complicated OEP equation can be cast into the simple form of a vanishing density shift. We discussed how the exact OEP can easily be calculated from only the occupied Kohn-Sham orbitals and their first-order shifts. The exact exchange potential was calculated for (all-electron) closed-shell atoms and three-dimensional (pseudopotential) sodium clusters. For the first time, not only the total energy but also Kohn-Sham eigenvalues were accurately calculated for three-dimensional systems from the exact OEP. We discussed different indicators for the accuracy of an OEP solution. The KLI approach is a rather good approximation for the ground-state properties of atoms and small sodium clusters. The relative errors it introduces, however, are considerably larger for the clusters than for the atoms. We further investigated the asymptotic behavior of the exact exchange potential of Kohn-Sham theory. For the non-spherical clusters, it shows pronounced "ridges" which are missing in the potentials of widely-used approximations like LDA. Finally, we calculated the static electric dipole polarizability for several sodium clusters and compared exact-exchange OEP to exact-exchange KLI and to LDA. The advantages of self-interaction-free exact exchange were demonstrated, and the need for a correlation functional to go with exact exchange stressed.

Our method greatly facilitates the self-consistent use of orbital functionals like the exact exchange energy in Kohn-Sham calculations. Orbital functionals can now be used fully self-consistently with moderate effort, and the accuracy of approximations to the OEP, such as KLI, can be checked. Due to the correct long-range asymptotics, functionals that use full exact exchange appear very promising for time-dependent DFT. The great influence that exact exchange has on the Kohn-Sham eigenvalues, which play a prominent role in time-dependent calculations, was demonstrated for the metal clusters. The locality of the Kohn-Sham potential is particularly beneficial in this context and makes Kohn-Sham theory

superior³⁶ to theories with orbital-dependent potentials, e.g., Hartree-Fock. Therefore, we believe that orbital functionals and the OEP method will play a prominent role in future functional development.

Acknowledgments

We are grateful to K. Burke for comments on the exact-exchange virial relation, and acknowledge discussions with M. Levy, J. Tao, E. Sagvolden, and D. Kolb. We thank J. Krieger for asking the question that is discussed in Appendix D. S.K. acknowledges financial support by the Deutsche Forschungsgemeinschaft under an Emmy-Noether grant, and J.P.P. by the U.S. National Science Foundation under grant DMR 01-35678.

APPENDIX A: THE ORBITAL ENERGY DENSITY FUNCTIONAL $E_v^{\text{orb},\alpha}[n]$

Our particular definition of the orbital functional $E_v^{\text{orb},\alpha}[n]$ was chosen to avoid problems that other rather natural-looking definitions may have. An intuitively plausible definition, e.g. could have required the orbitals to be orthogonal. However, it is known that certain orbital functionals, e.g., the SIC functional⁵⁰, are minimized by non-orthogonal orbitals. Requiring orthogonality in the definition of $E_v^{\text{orb},\alpha}[n]$ for the SIC would require non-trivial modifications of Eq. (14), e.g., introducing off-diagonal Lagrangian multipliers. On the other hand, simply dropping the orthogonality condition and requiring the orbitals to be just the ones minimizing the energy could lead to a "bosonic" solution, with all electrons occupying the lowest orbital. Therefore, in the definition of $E_v^{\text{orb},\alpha}[n]$ the orbitals are required to be linearly independent. They are further required to be extremizing ones and not just the ones yielding the lowest possible energy for a given density, because the latter criterion could be fulfilled by a "nearly bosonic" solution, with all electrons occupying orbitals that are extremely similar to the lowest one but with a tiny contribution added to each one of them to make them linearly independent. Our definition of $E_v^{\text{orb},\alpha}[n]$ raises a question similar to the questions of v -representability which are still a subject of current research in Kohn-Sham theory⁹⁹. In our case the question is: Can we find a set of orbitals that extremizes Eq. (9) for *any* given density? However, we believe that for our present purposes this question does not pose a problem because we are interested in the minimizing density, which we know can be obtained from Eq. (14).

Eq. (14) starts from a given external potential $v(\mathbf{r})$ and finds the orbitals and density belonging to it. If instead we want the $\varphi_i^{\text{orb},\alpha}[n]$ corresponding to a given density $n(\mathbf{r})$, we must add to $v(\mathbf{r})$ in Eq. (14) a Lagrange-multiplier $\Delta v([n]; \mathbf{r})$ which enforces the constraint of Eq. (10).

APPENDIX B: PROOF THAT THE MINIMIZING DENSITIES FOR $E_v^{\text{orb},\alpha}[n]$ AND $E_v^{\text{OEP},\alpha}[n]$ AGREE TO LINEAR ORDER IN α

In Eqs. (12) and (13), we defined the functionals $E_v^{\text{OEP},\alpha}[n]$ and $E_v^{\text{orb},\alpha}[n]$ by starting from Eq. (9) and its discussion. Assuming that $E_v^{\text{orb},\alpha}[n]$ is analytic in α , we consider the power series expansion

$$E_v^{\text{orb},\alpha}[n] = E_v^{\text{OEP},\alpha}[n] + \alpha A_1[n] + \alpha^2 A_2[n] + \dots \quad (\text{B1})$$

The analog of this expansion for the densities is

$$n^{\text{orb},\alpha}(\mathbf{r}) = n^{\text{OEP},\alpha}(\mathbf{r}) + \alpha n_1(\mathbf{r}) + \alpha^2 n_2(\mathbf{r}) + \dots \quad (\text{B2})$$

We also argued in Section II that

$$A_1[n] = 0. \quad (\text{B3})$$

Now rewrite the Euler equation for $n^{\text{orb},\alpha}(\mathbf{r})$:

$$\left. \frac{\delta E_v^{\text{orb},\alpha}[n]}{\delta n(\mathbf{r})} \right|_{n^{\text{orb},\alpha}} = 0 \quad (\text{B4})$$

$$= \left. \frac{\delta E_v^{\text{OEP},\alpha}[n]}{\delta n(\mathbf{r})} \right|_{n^{\text{orb},\alpha}} + \alpha^2 \left. \frac{\delta A_2[n]}{\delta n(\mathbf{r})} \right|_{n^{\text{orb},\alpha}} + \dots \quad (\text{B5})$$

$$= \left. \frac{\delta E_v^{\text{OEP},\alpha}[n]}{\delta n(\mathbf{r})} \right|_{n^{\text{OEP},\alpha} + \alpha n_1 + \dots} + \mathcal{O}(\alpha^2) \quad (\text{B6})$$

$$= \left. \frac{\delta E_v^{\text{OEP},\alpha}[n]}{\delta n(\mathbf{r})} \right|_{n^{\text{OEP},\alpha}} + \alpha \int \left. \frac{\delta^2 E_v^{\text{OEP},\alpha}[n]}{\delta n(\mathbf{r}) \delta n(\mathbf{r}')} \right|_{n^{\text{OEP},\alpha}} n_1(\mathbf{r}') d^3 r' + \mathcal{O}(\alpha^2) \quad (\text{B7})$$

Eq. (B5) follows from Eqs. (B1) and (B3). In Eq. (B6) we use Eq. (B2), and we can focus on the terms linear in α because each order of α must vanish separately. Eq. (B7) finally follows from functional Taylor expansion. The first term in (B7) is just the Euler equation for $n^{\text{OEP},\alpha}(\mathbf{r})$ and therefore vanishes. So

$$\int \left. \frac{\delta^2 E_v^{\text{OEP},\alpha}[n]}{\delta n(\mathbf{r}) \delta n(\mathbf{r}')} \right|_{n^{\text{OEP},\alpha}} n_1(\mathbf{r}') d^3 r' = 0, \quad (\text{B8})$$

and Eq. (B8) must be fulfilled for all α . Since the double functional derivative in Eq. (B8) depends upon α , while $n_1(\mathbf{r}')$ does not, Eq. (B8) can only be fulfilled by

$$n_1(\mathbf{r}) = 0, \quad (\text{B9})$$

i.e., the minimizing densities $n^{\text{orb},\alpha}(\mathbf{r})$ and $n^{\text{OEP},\alpha}(\mathbf{r})$ agree to linear order in α .

We can compute $n_1(\mathbf{r})$ from first-order perturbation theory. Since, from Eq. (B2),

$$\alpha n_1(\mathbf{r}) = n^{\text{orb},\alpha}(\mathbf{r}) - n^{\text{OEP},\alpha}(\mathbf{r}) + \mathcal{O}(\alpha^2), \quad (\text{B10})$$

$n_1(\mathbf{r})$ can be computed by evaluating the density change that is associated with going over from the OEP-functional to the orbital density functional and neglecting

all orders in α beyond the linear one. This density change can be calculated from the corresponding change in the single-particle orbitals. To this end, we rewrite Eq. (14) with the help of Eqs. (17) and (18) in the form

$$\left(-\frac{\hbar^2}{2m} \nabla^2 + v(\mathbf{r}) + v_{\text{H}}(\mathbf{r}) + \alpha v_{\text{xc}}(\mathbf{r}) \right) \varphi_i^{\text{orb},\alpha}(\mathbf{r}) + \alpha [u_{\text{xc}i}(\mathbf{r}) - v_{\text{xc}}(\mathbf{r})] \varphi_i^{\text{orb},\alpha}(\mathbf{r}) = \varepsilon_i^{\text{orb},\alpha} \varphi_i^{\text{orb},\alpha}(\mathbf{r}). \quad (\text{B11})$$

Clearly, if we neglect the term in brackets in the second line of Eq. (B11), we are looking at the Kohn-Sham system. Thus, we can calculate the shift that the orbitals undergo when we go over from the Kohn-Sham to the orbital density functional by treating $\alpha [u_{\text{xc}i}(\mathbf{r}) - v_{\text{xc}}(\mathbf{r})]$ as a perturbation on the Kohn-Sham system. In non-degenerate first-order perturbation theory (see Section II for remarks on the degenerate case), the shifted orbital is

$$\varphi_i^{\text{pert},\alpha}(\mathbf{r}) = \varphi_i^\alpha(\mathbf{r}) + \sum_{\substack{j=1 \\ j \neq i}}^{\infty} \frac{\langle \varphi_j^\alpha | \alpha [u_{\text{xc}i} - v_{\text{xc}}] | \varphi_i^\alpha \rangle}{\varepsilon_i - \varepsilon_j} \varphi_j^\alpha(\mathbf{r}), \quad (\text{B12})$$

where $\varphi_i^\alpha(\mathbf{r})$ and ε_i are the Kohn-Sham orbitals and eigenvalues corresponding to the minimizing density $n^{\text{OEP},\alpha}(\mathbf{r})$. The important fact to be noted here is that the perturbation is linear in α . Thus, higher orders of perturbation theory will also be of higher order in α . Since we want to calculate the change in density only to first order in α , only the orbital shift in first-order perturbation theory needs to be taken into account. We insert Eq. (B12) into Eq. (B10),

$$\begin{aligned} \alpha n_1(\mathbf{r}) &= \sum_{i=1}^N \varphi_i^{\text{pert},\alpha}(\mathbf{r}) \varphi_i^{\text{pert},\alpha*}(\mathbf{r}) - \sum_{i=1}^N \varphi_i^\alpha(\mathbf{r}) \varphi_i^{\alpha*}(\mathbf{r}) \\ &= \alpha \sum_{i=1}^N \varphi_i^\alpha(\mathbf{r}) \varphi_{i,1}^{\alpha*}(\mathbf{r}) + c.c. + \mathcal{O}(\alpha^2), \end{aligned} \quad (\text{B13})$$

where $\varphi_{i,1}^{\alpha}(\mathbf{r})$ is defined as the second term on the right-hand side of Eq. (B12) divided by α . Obviously, $\varphi_{i,1}^{\alpha=1}(\mathbf{r}) = -\psi_i(\mathbf{r})$, and thus Eq. (B9) is exactly Eq. (1).

APPENDIX C: NUMERICAL ASPECTS OF THE ITERATIVE CONSTRUCTION

In this Appendix we summarize some of the more technical details of the iterative solution of the OEP equation.

We first discuss the convergence of the iteration based on Eq. (23) for the exact-exchange-only OEP. The test system here is the Be atom. The Kohn-Sham equations were solved on a logarithmic radial grid. Table III illustrates how many iterations going back and forth between Eq. (4) and Eq. (23) are necessary for a given number of $(\psi_{i\sigma}^*, v_{\text{xc}\sigma})$ -cycles to converge the total energy and eigenvalues to the OEP values with an accuracy of 0.1 mhar. The starting point is the KLI potential. The total energy

is correct after one iteration in all cases (the difference is small to begin with), but also the eigenvalues which are noticeably different in KLI and OEP converge quickly: With just 5 $(\psi_{i\sigma}^*, v_{xc\sigma})$ -cycles per iteration, it takes only 5 iterations to reach the exact OEP. We also note that for the second and later iteration steps, the self-consistent solution of the Kohn-Sham equations proceeds much faster than the first self-consistent solution that is needed to get the starting approximation. This has two reasons. First, we need to recalculate the $u_{xc\sigma}$ only once at the beginning of each new $(\psi_{i\sigma}^*, v_{xc\sigma})$ -cycle and not at each step in the self-consistent solution of the Kohn-Sham equations (since v_{xc} is kept fixed during the latter). Second, the orbitals and shifts from the previous iteration are already a good starting guess for the next one. Therefore, the whole scheme converges very rapidly.

However, Eq. (23) requires dividing by the density, and this is a disadvantage if it is to be used for finite systems. The first term under the sum is unproblematic. It is asymptotically dominated by the highest occupied orbital which also dominates the density. Thus, even if the density in the denominator has decayed to the extent that its numerical representation becomes highly inaccurate, the same inaccuracies show up in the numerator, and the correct result is still obtained. This cancellation does not occur in the second or gradient term, and the resulting inaccuracies can make the scheme unstable. For spherical systems, the problem can easily be solved. In the asymptotic region, the KLI potential is already correct, therefore the second term need not be evaluated numerically there. And the asymptotic region for a spherical system can easily be identified by going out from the system's center and monitoring when the density starts to be dominated by the highest occupied orbital. In this way, calculations for spherical atoms can be done simply.

But the accuracy of the method depends rather sensitively on the cut-off point: With a cut-off too close to the system's center, too much of the second term is lost; with a cut-off that is too far away, the iteration becomes unstable. In the spherical, effectively one-dimensional calculations, the numerical parameters can be chosen such that finding an appropriate cut-off radius is possible. Our real

TABLE III: Number of iterations necessary to converge all eigenvalues of the Be atom to their exact OEP values $E = -14.5724$, $\varepsilon_1 = -4.1257$, $\varepsilon_2 = -0.3092$, for a given number of $(\psi_{i\sigma}^*, v_{xc\sigma})$ -cycles. The total energy is correct after one iteration. Starting point is the KLI approximation ($E = -14.5723$, $\varepsilon_1 = -4.1668$, $\varepsilon_2 = -0.3089$, all energies in hartree). Note that convergence is achieved with very moderate effort.

$(\psi_{i\sigma}^*, v_{xc\sigma})$ -cycles	iterations	$(\psi_{i\sigma}^*, v_{xc\sigma})$ -cycles	iterations
1	24	5	5
2	10	10	3
3	9	20	3

interest, however, is in non-spherical systems of possibly complex shape. We found that for three-dimensional (3D) systems, the technical difficulties are more severe. The coarser grids that computational necessity forces on us lead to larger inaccuracies in the evaluation of the derivatives that appear in the second term and allow for less fine tuning of the cut-off point. Furthermore, the asymptotic region will start at different distances in different directions and must be mapped out more carefully.

As a first test case for a 3D implementation of our algorithm, we chose the jellium cluster Na_8 . It is a good test case because it is spherical, i.e., the OEP can be obtained from the established direct solution of the integral equation for comparison³². But unlike the diverging atomic nuclear potential, jellium Na_8 can also be represented on the 3D Cartesian grid which we use for a realistic, pseudopotential-based description of metal clusters. The Seitz radius ($r_s = [3/(4\pi n)]^{1/3}$) of the jellium background density was $r_s = 3.93 a_0$, corresponding to a sphere of radius $7.86 a_0$. We first calculated the KLI approximation and compared a spherical, one-dimensional calculation on a logarithmic grid to a 3D calculation (Cartesian grid, 65 points in each direction, spacing $0.7a_0$, damped gradient iteration with finite-difference multigrid relaxation¹⁰⁰) that does not exploit the spherical symmetry. Both yield identical energies and eigenvalues to within 0.1 mhar. This confirms the accuracy of our 3D code. We then constructed the OEP iteratively on the same grid for different cut-off radii between $4 a_0$ and $19 a_0$. Only with cut-offs close to $6 a_0$ was the iteration unproblematic and converged to the correct total energy $E = -0.3735$ har. However, the lowest eigenvalue was still 0.4 mhar above its correct value 0.2081 har, i.e., halfway between the OEP and KLI values. Obtaining the OEP via Eq. (23) for the real, non-spherical clusters turned out to be even more complicated. The situation can be improved with finer grids, but using Eq. (23) in 3D calculations is rather tedious.

The iteration based on Eq. (26) does not suffer from these problems. The convergence is slower than for the first method, but the computational effort is still very moderate: For the test system jellium Na_8 , the total energy and all eigenvalues converge within 5 iterations if 10 cycles are used. With Eq. (26), the 3D calculation now also yields exactly the same energy and eigenvalues as the spherical, direct solution of the OEP integral equation^{25,32}. During the iterations, the relative error in the exchange virial relation falls by two orders of magnitude compared to the KLI approximation, and S_{\max} decreases to 2×10^{-6} . Further iterations reduce both quantities further. Thus, the simple iteration very accurately yields the exact OEP also for 3D systems.

The parameter c used in the iteration was chosen by trial and error. If c is chosen too large, the iteration diverges, and with c too small, it does not converge as quickly as possible. In all cases we studied, finding appropriate values for c was unproblematic and there was a range of suitable values. We used c 's between $3 \text{ har } a_0^3$

and $0.75 \text{ har } a_0^3$ for the atoms, and $c=30 \text{ har } a_0^3$ for all the cluster calculations. Thus, c was similar for similar systems, i.e., c 's of about 1 were appropriate for the atoms with their singular nuclear potential, and larger c 's could be used for the non-singular pseudopotential calculations.

These values can be understood on the basis of Eq. (28). For Na_4 , e.g., $-v_{x\sigma}(\mathbf{r})/(2n_\sigma(\mathbf{r}))$ takes values between $30 \text{ har } a_0^3$ and $40 \text{ har } a_0^3$ in the interior region of the cluster. A yet simpler and charming argument can be made based on the bulk limit. For a homogenous system, $-v_x/n = (9\pi/4)^{(1/3)}r_s^2 \text{ har } a_0 \approx 1.92 r_s^2 \text{ har } a_0$. For bulk sodium, $r_s = 3.93 a_0$, so $-v_x/n \approx 30 \text{ har } a_0^3$, and for atoms, the average density is about $r_s = 1 a_0$, so $-v_x/n$ is about $2 \text{ har } a_0^3$. These estimates agree nicely with the values we found by trial-and-error. Finally, we want to remark that the iteration could also be used with some suitably chosen $c(\mathbf{r})$, but for our present purposes a constant was satisfactory.

APPENDIX D: ON THE DIFFERENCE BETWEEN KLI AND OEP ORBITAL SHIFTS

Looking at Fig. 1, one might ask the following question: The KLI and OEP orbitals are rather similar. Therefore,

in Eq. (21) the operator on the left-hand side and all quantities on the right-hand side should be similar, too. But then, also the orbital shifts that are calculated from Eq. (21) should be similar. So how can it be that we observe the pronounced difference between the KLI and OEP orbital shift $\psi_1(\mathbf{r})$ shown in the lowest part of Fig. 1?

The answer to this question is that although the Kohn-Sham orbitals obtained from the KLI potential and the OEP are similar, the respective right-hand sides in Eq. (21) nevertheless show a qualitative difference. The higher Kohn-Sham orbital $\varphi_2(\mathbf{r})$ has a nodal surface in the x-y plane, i.e., its orbital density vanishes there. Therefore, in this plane the KLI potential is just given by $u_{x1}(\mathbf{r}) - (\bar{v}_{x1} - \bar{u}_{x1})$. If this is inserted for $v_x(\mathbf{r})$ in the right-hand side of Eq. (21), the right-hand side vanishes. But for the OEP, there is an additional contribution to $v_x(\mathbf{r})$ from the term of Eq. (23) that involves the derivatives of the Kohn-Sham orbitals and their orbital shifts, and this term makes a non-vanishing contribution in the x-y plane. The qualitative difference between OEP and KLI orbital shift is thus a direct consequence of a qualitative difference of the respective right-hand sides in Eq. (21).

-
- ¹ P. Hohenberg and W. Kohn, Phys. Rev. **136**, B864 (1964).
² W. Kohn and L. J. Sham, Phys. Rev. **140**, A 1133 (1965).
³ J. P. Perdew, Phys. Rev. Lett. **55**, 1665 (1985).
⁴ A. D. Becke, Phys. Rev. A **38**, 3098 (1988).
⁵ C. Lee, W. Yang, and R. G. Parr, Phys. Rev. B **37**, 785 (1988).
⁶ J. P. Perdew, K. Burke, and M. Ernzerhof, Phys. Rev. Lett. **77**, 3865 (1996).
⁷ J. P. Perdew and K. Schmidt, in *Density Functional Theory and Its Applications to Materials*, edited by V. VanDoren, K. VanAlsenoy, and P. Geerlings (American Institute of Physics, 2001).
⁸ A. D. Becke, J. Chem. Phys. **98**, 1372 (1993); J. Chem. Phys. **107**, 8554 (1997).
⁹ J. P. Perdew, M. Ernzerhof, and K. Burke, J. Chem. Phys. **105**, 9982 (1996).
¹⁰ M. Ernzerhof, J. P. Perdew, and K. Burke, Int. J. Quantum Chem. **64**, 285 (1997).
¹¹ K. Burke, M. Ernzerhof, J. P. Perdew, Chem. Phys. Lett. **265**, 115 (1997).
¹² M. Ernzerhof and G. E. Scuseria, J. Chem. Phys. **110**, 5029 (1999).
¹³ J. Jaramillo, G. E. Scuseria, and M. Ernzerhof, J. Chem. Phys. **118**, 1068 (2003).
¹⁴ J. P. Perdew, J. Tao, S. Kümmel, K. Schmidt, V. Straroverov, and G. E. Scuseria, work in progress.
¹⁵ J. P. Perdew and S. Kurth, in *Density Functionals: Theory and Applications*, edited by D. P. Joubert (Springer Lecture Notes in Physics, Springer, Berlin, 1998).
¹⁶ F. Della Sala and A. Görling, Phys. Rev. Lett. **89**, 33003 (2002); J. Chem. Phys. **116**, 5374 (2002).
¹⁷ A. R. Goñi, U. Haboek, C. Thomsen, K. Eberl, F. A. Reboredo, C. R. Proetto, and F. Guinea, Phys. Rev. B **65**, 121313 (2002).
¹⁸ M. Städele, J. A. Majewski, P. Vogl, and A. Görling, Phys. Rev. Lett. **79**, 2089 (1997).
¹⁹ M. Städele, M. Moukara, J. A. Majewski, P. Vogl, and A. Görling, Phys. Rev. B **59**, 10031 (1999).
²⁰ D. M. Bylander and L. Kleinman, Phys. Rev. Lett. **74**, 3660 (1995).
²¹ Y.-H. Kim and A. Görling, Phys. Rev. Lett. **89**, 96402 (2002).
²² S. J. A. van Gisbergen, P. R. T. Schipper, O. V. Gritsenko, E. J. Baerends, J. G. Snijders, B. Champagne, and B. Kirtman, Phys. Rev. Lett. **83**, 694 (1999).
²³ S. Kümmel and J. P. Perdew, Phys. Rev. Lett. **90**, 043004 (2003).
²⁴ R. T. Sharp and G. K. Horton, Phys. Rev. **90**, 317 (1953).
²⁵ J. D. Talman and W. F. Shadwick, Phys. Rev. A **14**, 36 (1976).
²⁶ V. Sahni, J. Gruenebaum, and J. P. Perdew, Phys. Rev. B **26**, 4371 (1982).
²⁷ S. Kümmel and J. P. Perdew, to appear in Mol. Phys. An example of a functional that is too radically nonlocal is the Fermi-Amaldi energy discussed in Ref. 50.
²⁸ J. P. Perdew, S. Kurth, A. Zupan, and P. Blaha, Phys. Rev. Lett. **82**, 2544 (1999).
²⁹ J. Tao and J. P. Perdew, unpublished.
³⁰ J. B. Krieger, Y. Li, and G. J. Iafrate, Phys. Rev. A **46**, 5453 (1992).
³¹ E. Engel and S. H. Vosko, Phys. Rev. A **47**, 2800 (1993).
³² E. Engel and S. H. Vosko, Phys. Rev. B **50**, 10498 (1994).
³³ T. Kotani, Phys. Rev. B **50**, 14816 (1994).
³⁴ T. Kotani and H. Akai, Phys. Rev. B **54**, 16502 (1996).

- ³⁵ T. Grabo, T. Kreibich, and E. Gross, *Molecular Engineering* **7**, 27 (1997).
- ³⁶ T. Grabo, T. Kreibich, S. Kurth, and E. Gross, in *Strong Coulomb Correlation in Electronic Structure: Beyond the Local Density Approximation*, edited by V. Anisimov, (Gordon & Breach, Tokyo, 2000).
- ³⁷ A. Görling and M. Levy, *Phys. Rev. A* **50**, 196 (1994).
- ³⁸ A. Görling, *Phys. Rev. Lett.* **83**, 5459 (1999).
- ³⁹ S. Ivanov, S. Hirata, and R. J. Bartlett, *Phys. Rev. Lett.* **83**, 5455 (1999).
- ⁴⁰ S. Hirata, S. Ivanov, I. Grabowski, R. Bartlett, K. Burke, and J. Talman, *J. Chem. Phys.* **115**, 1635 (2001).
- ⁴¹ F. Della Sala and A. Görling, *J. Chem. Phys.* **115**, 5718 (2001).
- ⁴² S. Hamel, M. E. Casida, and D. R. Salahub, *J. Chem. Phys.* **116**, 8276 (2002).
- ⁴³ L. Fritsche and J. Yuan, *Phys. Rev. A* **57**, 3425 (1998).
- ⁴⁴ R. Colle and R. K. Nesbet, *J. Phys. B* **34**, 2475 (2001).
- ⁴⁵ W. Yang and Q. Wu, *Phys. Rev. Lett.* **89**, 143002 (2002).
- ⁴⁶ C. Calvayrac, P.-G. Reinhard, E. Suraud, and C. A. Ullrich, *Phys. Rep.* **337**, 493 (2000).
- ⁴⁷ L. Kronik, I. Vasiliev, M. Jain, and J. R. Chelikowsky, *J. Chem. Phys.* **115**, 4322 (2001).
- ⁴⁸ T. L. Beck, *Rev. Mod. Phys.* **72**, 1041 (2001).
- ⁴⁹ With this choice for $u_{xc}(\mathbf{r})$, Eq. (1) is the first of a series of equations which assert that the density does not change to *any* order of many-body perturbation theory along the adiabatic connection, see A. Görling and M. Levy, *Int. J. Quantum Chem. S* **29**, 93 (1995).
- ⁵⁰ J. P. Perdew and A. Zunger, *Phys. Rev. B* **23**, 5048 (1981).
- ⁵¹ C. Legrand, E. Suraud, and P.-G. Reinhard, *J. Phys. B* **35**, 1 (2002).
- ⁵² V. R. Shaginyan, *Phys. Rev. A* **47**, 1507 (1993).
- ⁵³ E. Engel and R. M. Dreizler, *J. Comp. Chem.* **20**, 31 (1999).
- ⁵⁴ S. Ivanov and M. Levy, *J. Chem. Phys.* **116**, 6924 (2002).
- ⁵⁵ M. Levy, *Proc. Natl. Acad. Sc. USA* **76**, 6062 (1979).
- ⁵⁶ R. M. Dreizler and E. K. U. Gross, *Density Functional Theory* (Springer, Berlin 1990).
- ⁵⁷ A. Holas, N. H. March, Y. Takahashi, and C. Zhang, *Phys. Rev. A* **48**, 2709 (1993).
- ⁵⁸ D. C. Langreth and J. P. Perdew, *Solid State Commun.* **17**, 1425 (1975).
- ⁵⁹ O. Gunnarsson and B. I. Lundqvist, *Phys. Rev. B* **13**, 4274 (1976).
- ⁶⁰ V. Sahni and M. Levy, *Phys. Rev. B* **33**, 3869 (1986).
- ⁶¹ E. K. U. Gross, M. Petersilka, and T. Grabo, in *Chemical Applications of Density Functional theory*, edited by B. B. Laird, R. B. Ross and T. Ziegler (ACS Symposium Series 629, 1996).
- ⁶² D. C. Langreth and M. J. Mehl, *Phys. Rev. B* **28**, 1809 (1983).
- ⁶³ M. Levy, J. P. Perdew, and V. Sahni, *Phys. Rev. A* **30**, 2745 (1984).
- ⁶⁴ C.-O. Almbladh and U. von Barth, *Phys. Rev. B* **31**, 3231 (1985).
- ⁶⁵ J. P. Perdew and M. Levy, *Phys. Rev. B* **56**, 16021 (1997).
- ⁶⁶ J. Chen, J. B. Krieger, R. O. Esquivel, M. J. Stott, and G. J. Iafrate, *Phys. Rev. A* **54**, 1910 (1996).
- ⁶⁷ I. Lindgren and J. Morrison, *Atomic Many Body Theory* (Springer-Verlag, Berlin, 1982).
- ⁶⁸ See, e.g., W. H. Press *et al.*, *Numerical Recipes in FORTRAN* (Cambridge University Press, 1992).
- ⁶⁹ R. M. Sternheimer, *Phys. Rev.* **96**, 951 (1954).
- ⁷⁰ S. Baroni, P. Giannozzi, and A. Testa, *Phys. Rev. Lett.* **58**, 1861 (1987).
- ⁷¹ M. Levy and J. P. Perdew, *Phys. Rev. A* **32**, 2010 (1985).
- ⁷² Y. Wang, J. P. Perdew, J. A. Chevary, L. D. Macdonald, and S. H. Vosko, *Phys. Rev. A* **41**, 78 (1990).
- ⁷³ J. P. Perdew and Y. Wang, *Phys. Rev. B* **45**, 13244 (1992).
- ⁷⁴ S. Kümmel, T. Berkus, P.-G. Reinhard, and M. Brack, *Eur. Phys. J. D* **11**, 239 (2000).
- ⁷⁵ S. Kümmel, M. Brack, and P.-G. Reinhard, *Phys. Rev. B* **62**, 7602 (2000); *ibid.* **63**, 129902 (2001) (E).
- ⁷⁶ A physically-motivated approximation to the exchange potential was given by M. K. Harbola and V. Sahni, *Phys. Rev. Lett.* **62**, 489 (1989), and stimulated some of the current interest in OEP.
- ⁷⁷ J. P. Perdew, R. G. Parr, M. Levy, and J. L. Balduz, Jr., *Phys. Rev. Lett.* **49**, 1691 (1982), and references therein.
- ⁷⁸ J. B. Krieger, Y. Li, and G. J. Iafrate, *Phys. Rev. A* **45**, 101 (1992).
- ⁷⁹ O. V. Gritsenko and E. J. Baerends, *Phys. Rev. A* **54**, 1957 (1996).
- ⁸⁰ I. Moullet, J. L. Martins, F. Reuse, and J. Buttet, *Phys. Rev. Lett.* **65**, 476 (1990); *Phys. Rev. B* **42**, 11598 (1990).
- ⁸¹ J. M. Pacheco and W. Ekardt, *Z. Phys. D* **24**, 65 (1992).
- ⁸² M. Madjet, C. Guet, and W. R. Johnson, *Phys. Rev. A* **51**, 1327 (1995).
- ⁸³ J. Guan, M. E. Casida, A. M. Köster, and D. R. Salahub, *Phys. Rev. B* **52**, 2184 (1995).
- ⁸⁴ J. A. Alonso and N. A. Cordero, in *Recent Developments and Applications of Modern Density Functional Theory*, ed. J. M. Seminario (Elsevier, Amsterdam, 1996).
- ⁸⁵ I. Vasiliev, S. Ögüt, and J. R. Chelikowsky, *Phys. Rev. Lett.* **82**, 1919 (1999).
- ⁸⁶ C. A. Ullrich, P.-G. Reinhard, and E. Suraud, *Phys. Rev. A* **62**, 053202 (2000).
- ⁸⁷ M. A. L. Marques, A. Castro, and A. Rubio, *J. Chem. Phys.* **115**, 3006 (2001).
- ⁸⁸ S. J. A. van Gisbergen, J. M. Pacheco, and E. J. Baerends, *Phys. Rev. A* **63**, 063201 (2001).
- ⁸⁹ W. D. Knight, K. Clemenger, W. A. de Heer, and W. A. Saunders, *Phys. Rev. B* **31**, 2539 (1985).
- ⁹⁰ D. Rayane, A. R. Allouche, E. Benichou, R. Antoine, M. Aubert-Frecon, Ph. Dugourd, M. Broyer, C. Ristori, F. Chandezon, B. A. Huber, and C. Guet, *Eur. Phys. J. D* **9**, 243 (1999).
- ⁹¹ G. Tikhonov, V. Kasperovich, K. Wong, and V. V. Kresin, *Phys. Rev. A* **64**, 063202 (2001).
- ⁹² S. Kümmel, J. Akola, and M. Manninen, *Phys. Rev. Lett.* **84**, 3827 (2000).
- ⁹³ L. Kronik, I. Vasiliev, and J. R. Chelikowsky, *Phys. Rev. B* **62**, 9992 (2000).
- ⁹⁴ S. A. Blundell, C. Guet, and R. R. Zope, *Phys. Rev. Lett.* **84**, 4826 (2000).
- ⁹⁵ D. M. Bylander and L. Kleinman, *Phys. Rev. B* **54**, 7891 (1996).
- ⁹⁶ D. M. Bylander and L. Kleinman, *Phys. Rev. B* **52**, 14566 (1995).
- ⁹⁷ A. Höck and E. Engel, *Phys. Rev. A* **58**, 3578 (1998).
- ⁹⁸ J. Tao and J. P. Perdew, work in progress.
- ⁹⁹ C. A. Ullrich and W. Kohn, *Phys. Rev. Lett.* **89**, 156401 (2002).
- ¹⁰⁰ S. Kümmel, *Structural and Optical Properties of Sodium Clusters studied in Density Functional Theory*, (Logos Verlag, Berlin, 2000).